

Direct observation of phase transitions in aluminate sodalite, $\text{Ca}_8[\text{Al}_{12}\text{O}_{24}](\text{CrO}_4)_2$

ISHMAEL HASSAN

Department of Geology, Faculty of Science, University of Kuwait, Safat 13060, Kuwait

ABSTRACT

Transmission electron microscopy (TEM) was used to study the structural changes that occur in aluminate sodalite, $\text{Ca}_8[\text{Al}_{12}\text{O}_{24}](\text{CrO}_4)_2$, when it is heated with the electron beam. Initially, a twinned orthorhombic crystal was heated, and it transformed to tetragonal and then to cubic symmetry. The cubic phase contains two-dimensional periodic antiphase boundaries (APBs) along the $\{110\}$ planes. The APBs are about 54 Å apart. Structural modulations also occurred during the transformations. The transition from tetragonal to orthorhombic symmetry is also associated with random transformation twins on a $\{110\}$ plane; this plane is both the composition and twin plane.

INTRODUCTION

Transmission electron microscopy (TEM) was used to study an aluminate sodalite, $\text{Ca}_8[\text{Al}_{12}\text{O}_{24}](\text{CrO}_4)_2$, with pseudocubic cell parameter $a = 9.222(2)$ Å and transition temperatures of 432, 453, and 610 K (Depmeier 1988a). This paper reports on cluster ordering, two-dimensional periodic antiphase boundaries (APBs), modulated structures, and, in particular, a series of transitions from cubic to orthorhombic superstructure with decreasing temperature. Other structural features and detailed previous works are described elsewhere (Hassan 1996a, 1996b, 1996c, 1996d).

Aluminate sodalites, $\text{M}_8[\text{Al}_{12}\text{O}_{24}](\text{XO}_4)_2$, with $\text{M} = \text{Ca}$, Sr , etc., and $\text{X} = \text{S}$, Cr , Mo , W , etc., form a technologically important family of compounds. Unusual properties of the compounds in the system include (1) ferroic phase transitions that create ferroelectric and ferroelastic species, (2) modulated structures and superstructures, (3) the possible existence of tricritical phase-transition behavior, and (4) strong framework-cluster interactions that induce structural strains (e.g., Depmeier et al. 1987; Depmeier 1988a, 1988b). The aluminate sodalites are stoichiometric, and the cage clusters are chemically identical $[\text{M}_4\text{XO}_4]^{6+}$. Moreover, in the cubic high-temperature phases, the XO_4 groups are disordered over six orientations (see Fig. 2 of Depmeier 1988a), and the transition to lower temperature tetragonal and orthorhombic phases is triggered by ordering of the XO_4 groups over less than six positions (Depmeier 1988a, 1988b). The M atom is bonded to one or two O atoms of the XO_4 group. Thus, there are essentially two coordinations for the $[\text{M}_4\text{XO}_4]^{6+}$ clusters, and they have different distributions of electron density.

The variety of chemistries and orientations of interstitial tetrahedral anion groups (e.g., SO_4^{2-} , CrO_4^{2-} , WO_4^{2-} , etc.) may result in the complex satellite reflections observed in diffraction patterns of sodalite (e.g., Hassan and Grundy 1984, 1989, 1991; Hassan et al. 1985; Hassan

and Buseck 1989a, 1989b; Xu and Veblen 1995). However, the origins of the satellite reflections are not known in detail.

TRANSITIONS IN ALUMINATE SODALITE

Selected-area electron diffraction (SAED) patterns and high-resolution transmission electron microscopy (HRTEM) data were recorded from crushed crystals deposited on holey carbon support films and by using various microscopes (see Hassan 1996a).

Structural changes may be discerned in HRTEM images of aluminate sodalite in the $[110]$ direction as a function of irradiation time (Fig. 1). Few s_1 modulated fringes are seen in Figure 1a, but numerous such fringes occur in Figure 1b, which was recorded several seconds later. These modulated fringes are parallel to the $(1\bar{1}0)$ planes, and they were induced by heating the sample with the electron beam. The corresponding SAED pattern after heating is shown in Figure 2. The main reflections can be classified into two groups: One group of strong reflections obeys the constraints imposed by body-centered symmetry and is called type p ($hkl: h + k + l = 2n$); and a second group of weaker reflections violates the systematic absences imposed by the body centering and is called type p' ($hkl: h + k + l = 2n + 1$). Additional reflections occur midway between substructure spots along $\langle 110 \rangle^*$ directions and are denoted r . When the r reflections are split along $\langle 110 \rangle^*$, they are denoted r_s . The s satellite reflections (i.e., s_1 and s_2) occur along $\langle 110 \rangle^*$ on either side of the main p spots. The s satellite reflections are streaked along $\langle 110 \rangle^*$. Both the r_s and s satellite reflections correspond to a periodicity of 53.5 Å. The x -like q satellite reflections are streaked parallel to $\langle 112 \rangle^*$, and they are similar to satellite reflections observed in nosean and hauyne (Hassan and Buseck 1989a, 1989b). Lastly, extra superstructure reflections occur along c^* , indicating a doubling among the $(00l)$ planes (Fig. 2; top unlabeled arrow).

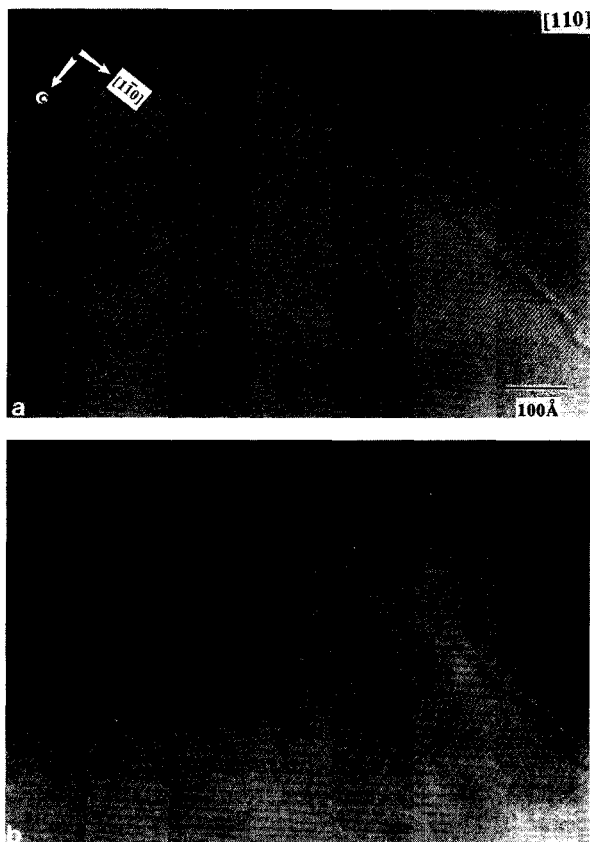


FIGURE 1. Transformations in the [110] image of aluminate sodalite. Few s_1 modulated fringes occur in **a**, but numerous such fringes occur in **b**, which was recorded several seconds later. The modulated fringes are parallel to a {110} plane. The periodicity of the s_1 modulated fringes is about 54 Å.

A twin boundary parallel to a (110) plane is visible in the [001] image of the orthorhombic aluminate sodalite (Fig. 3). In the Figure, parts a and b of the crystal are twin domains separated by a twin boundary as indicated by the double-headed arrow. A detailed discussion of twinning in aluminate sodalite was given by Hassan (1996a). The orthorhombic supercell in both parts of the twin crystal has $2a \times 3b \times c$ parameters (Fig. 4). The structure observed in Figure 3 was transformed by electron-beam heating to that shown in Figure 5. The electron beam was placed on the b twin component such that the a component remained relatively unchanged because it was resting close to the carbon film (upper right). The transformation began at the twin boundary, presumably because of the strain energy localized along the boundary. The letters a–e correspond to the same regions in both images (Figs. 3 and 5), and the optical diffractograms (Figs. 6a–6d; the optical diffractogram corresponding to area e is given in the Fig. 5 inset) are from the corresponding areas after beam heating. The optical diffractograms were obtained by passing a laser beam (diameter

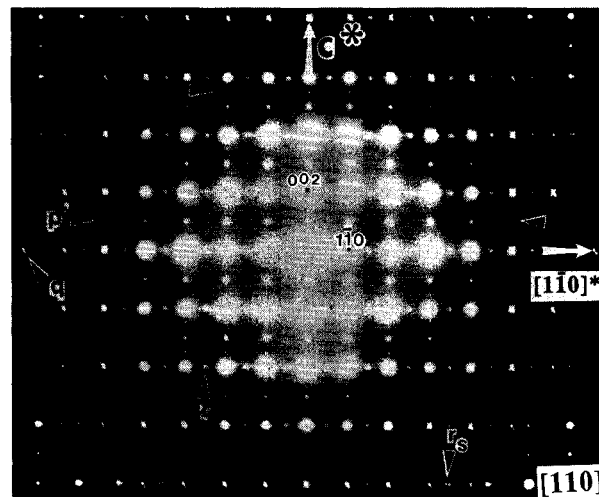


FIGURE 2. The [110] SAED pattern corresponding to the image shown in Figure 1 after heating. The q , r , and r_s reflections are shown. Note the divergence of q satellite reflections toward the edges.

≈ 0.5 cm) through the image negative. The optical diffractograms are very useful in following the phase transitions because of the small area being analyzed. An SAED pattern from the area shown in Figure 5 is very complicated because three distinct phases are present, and the modulations are not easily unraveled from a composite diffraction pattern.

The twin boundary shown in Figure 3 is indicated by a double-headed arrow in Figure 5. Region a contained $2a \times 3b$ fringes (Fig. 3) throughout the transformation (Fig. 5), as indicated also by the corresponding optical diffractogram (Fig. 6a). A detailed description of the orthorhombic superstructure with supercell parameters of $2a \times 3b \times c$ can be found elsewhere (Hassan 1996c).

Regions b and c contain modulated fringes (Fig. 5), as indicated also by the corresponding optical diffractograms (Figs. 6b and 6c, respectively). The modulations occur along b^* (see optical diffractograms). A detailed description of the modulated structure was given elsewhere (Hassan 1996b).

Region d contains two-dimensional periodic APBs at right angles to each other (Fig. 5; arrows), as indicated by the optical diffractogram (Fig. 6d). Pairs of r_s reflections at 90° angles to each other indicate two-dimensional periodic APBs (Fig. 6d). A detailed description of the two-dimensional periodic APBs can be found elsewhere (Hassan 1996d).

Region e has tetragonal symmetry (Fig. 5), as indicated by the optical diffractogram (inset). The tetragonal supercell parameters are $(a + b) \times (-a + b) \times c$ (i.e., $2d_{110} \times 2d_{\bar{1}10} \times c$). A detailed description of the tetragonal superstructure was given elsewhere (Hassan 1996c).

A comparison of the optical diffractograms in Figure 6d and the Figure 5 inset reveals the path of the transition

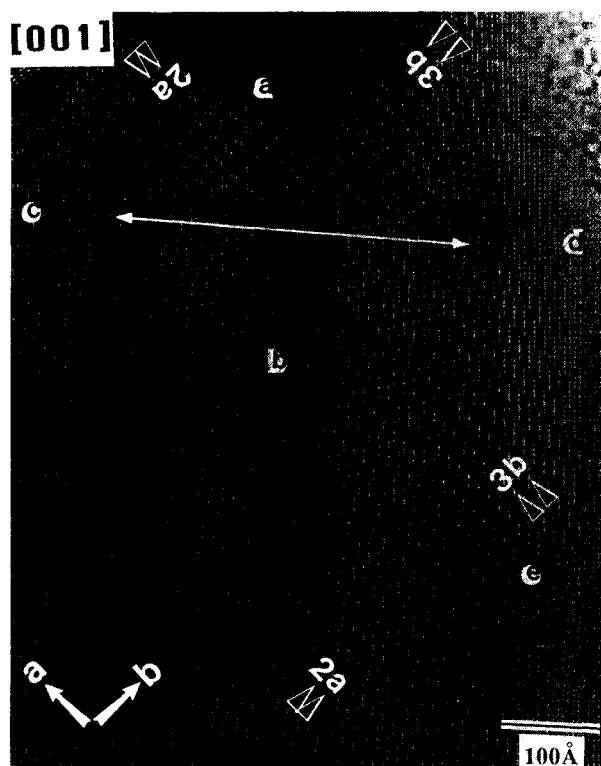


FIGURE 3. The [001] image showing twinning in aluminite sodalite. Regions a and b of the crystal are related by the twin boundary indicated by the double-headed arrow that is parallel to the (110) plane. The supercell parameters of both parts of the twin crystal are $2a \times 3b \times c$. This crystal was later transformed to that shown in Figure 5. The regions labeled a–e correspond to those shown in Figure 5.

from cubic to tetragonal symmetry: The split r reflections (Fig. 6d) coalesced to form a single spot (Fig. 5 inset), and the weak p' reflections in Figure 6d occur as stronger reflections in the Figure 5 inset. The optical diffractograms indicate a cubic structure with APBs (Fig. 6d), a tetragonal cell with parameters of $(a + b) \times (-a + b) \times c$ (Fig. 5 inset), and an orthorhombic cell with parameters of $2a \times 3b \times c$ (Fig. 6a). In all cases, the c parameter was inferred because it was not observed in these projections, but the results are consistent with numerous observations in other directions (Hassan 1996a, 1996b, 1996c, 1996d).

The phase transitions occurred in the aluminite sodalite because of the electron-beam heating. This process produced a temperature gradient across the sample. Initially, the twinned single-crystal fragment had orthorhombic symmetry that changed to tetragonal and subsequently to cubic symmetry. The electron beam was placed on areas b and d, so the cubic phase occurred between the orthorhombic and the tetragonal phases because of the temperature gradient (Fig. 5). The transitions occurred through structural modulations, but it is not clear whether these modulations accompanied one or both of the tran-

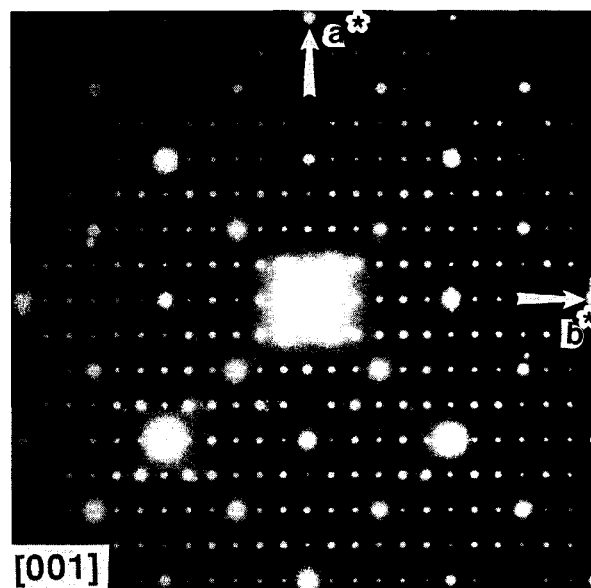


FIGURE 4. The [001] SAED pattern of the twinned crystal shown in Figure 3. The orthorhombic supercell parameters are $2a \times 3b \times c$.

sitions (orthorhombic to tetragonal, and tetragonal to cubic). Nevertheless, the image clearly illustrates that structural modulations occur during the transition from one structural state to another. The cubic phase contains the two-dimensional periodic APBs that are discussed in detail elsewhere (Hassan 1996d).

DISCUSSION

If the AlO_4 tetrahedra in the aluminite sodalites are regular and of the same size and the framework is fully expanded, the space group of the aluminite sodalites is $Im\bar{3}m$. If the tetrahedra are rotated, the symmetry remains cubic, but the space group changes from $Im\bar{3}m$ to $I\bar{4}3m$. In the case of the aluminosilicate sodalites, the ordering of Al and Si atoms leads to a further reduction in symmetry to $P\bar{4}3n$; which is the average space group of nosean (see Hassan and Grundy 1984, 1989). The weak p' reflections imply that the $[\text{Ca}_4\text{CrO}_4]^{6+}$ clusters within the cages centered at $(0,0,0)$ and $(\frac{1}{2}, \frac{1}{2}, \frac{1}{2})$ are not equivalent. Nosean contains p' reflections and random APBs that are based on cluster ordering. In the case of nosean, the p' reflections indicate that space group $P23$, a subgroup of $P\bar{4}3n$, is most appropriate for the individual domains in nosean. A model structure for nosean in space group $P23$ was given by Hassan and Grundy (1989). The space group is $I\bar{4}3m$ for the high-temperature cubic aluminite sodalite, but the APBs and p' reflections indicate that the space group for the modulated structure is probably $P23$ or lower.

The calculated HRTEM images of nosean indicate that ordered $[\text{Na}_4\text{SO}_4]^{2+}$ and $[\text{Na}_4\text{H}_2\text{O}]^{4+}$ clusters can be recognized by HRTEM imaging, and this ordering was ex-

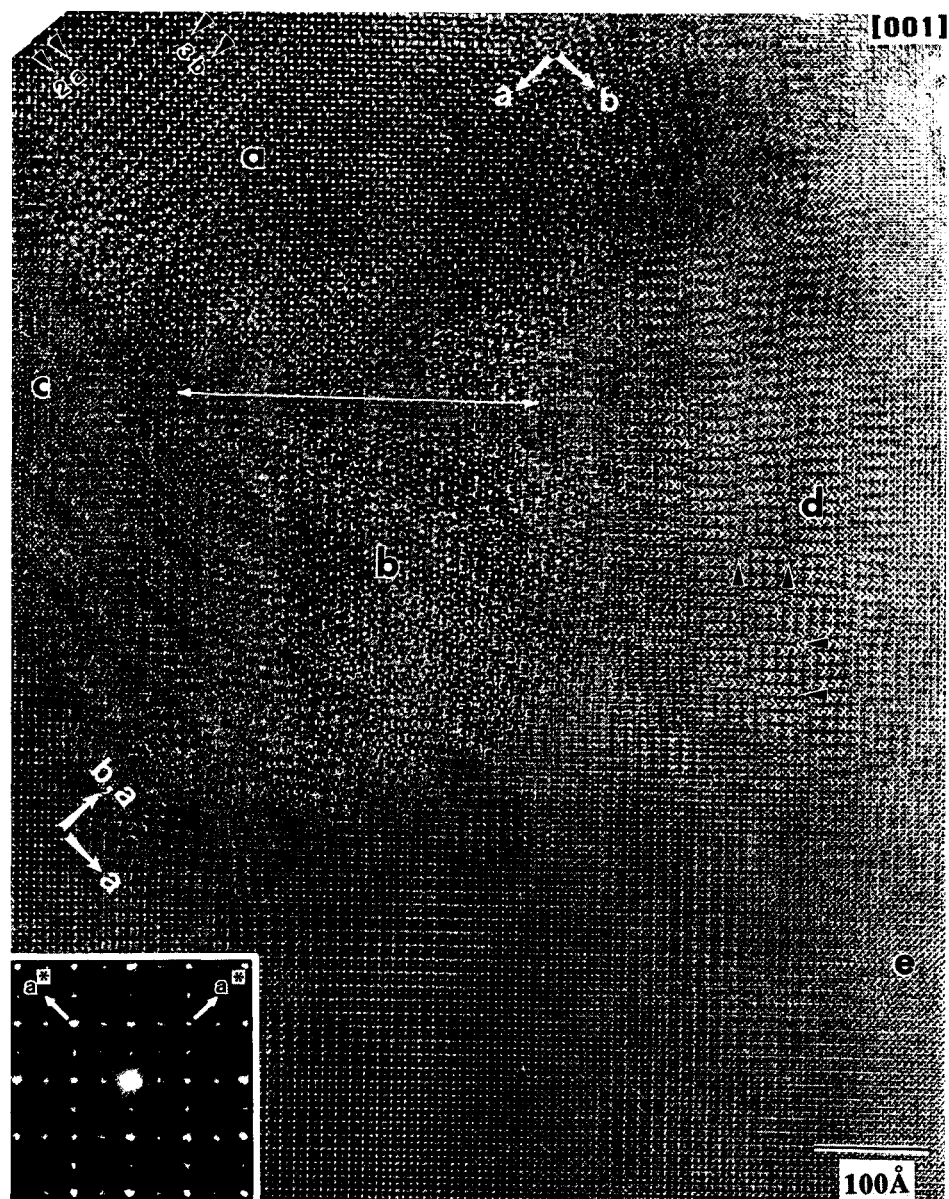


FIGURE 5. The [001] image of aluminite sodalite after transformation. The twin boundary is indicated by the double-headed arrow. Region a contains a $2a \times 3b$ supercell that did not change during the transformations. Regions b and c contain modulated fringes, region d contains two-dimensional periodic APBs (pairs of arrows), and region e is a product of the transformation and has tetragonal symmetry, as indicated by the optical diffractogram (inset).

perimentally observed as differences in contrast along (100) and (200), and (010) and (020) planes, respectively (Hassan and Buseck 1989a, 1989b). This ordering of clusters causes random APBs in nosean and hauyne, analogous to those in scapolite-group minerals (Hassan and Buseck 1988, 1989a, 1989b). In nosean, if the cavity at (0,0,0) is occupied by $[\text{Na}_4\cdot\text{SO}_4]^{2+}$ clusters, then the cavity at $(\frac{1}{2}, \frac{1}{2}, \frac{1}{2})$ is occupied by $[\text{Na}_4\cdot\text{H}_2\text{O}]^{4+}$ clusters; in the adjacent domain the occupancy of the cavities is reversed. In the case of the aluminite sodalite, cluster ordering with

six orientations occurs in the cubic phase, but it leads to two-dimensional periodic APBs (see Hassan 1996d). The alternating light and dark fringes shift back and forth, both horizontally and vertically, by one-half the (110) spacing across the APBs (Fig. 5). The alternating light and dark fringes indicate ordering of $[\text{Ca}_4\cdot\text{CrO}_4]^{6+}$ clusters. Differences in contrast are also seen along the (100) and (200), and (010) and (020) planes (see Fig. 5).

SAED patterns indicate that the aluminite sodalite structure is modulated in several directions, notably

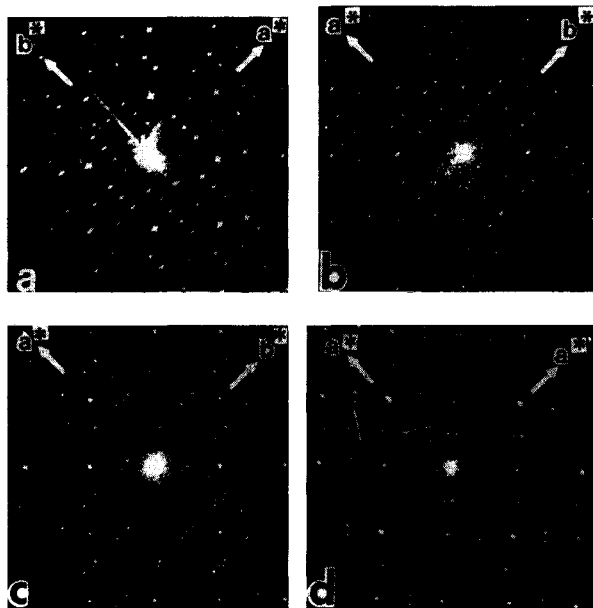


FIGURE 6. Optical diffractograms of the regions shown in the $[001]$ image of aluminatesodalite (Fig. 5). Diffractograms **a–d** correspond to the regions labeled **a–d** in Figure 5. A $2a \times 3b$ supercell is shown in **a**, **b** and **c** indicate modulations along b^* , and the arrows in **d** point to r_s reflections that cause the two-dimensional periodic APBs.

$\langle 100 \rangle^*$, $\langle 110 \rangle^*$, and $\langle 112 \rangle^*$. The TEM images of the aluminatesodalite show that the structure is modulated in several directions in different parts of the crystal, and some parts are unmodulated. In the modulated parts, the framework O atoms are positionally ordered on the O1 and O2 positions, whereas in unmodulated parts they are presumably disordered (see Hassan 1996b). The disordered domains may be compared with a high-temperature cubic phase, and the ordered domains can be considered analogous to a cubic phase that is in a transitional state. The modulations of the framework O atoms cause the satellite reflections (Hassan 1996b). However, a structure refinement is necessary to determine if indeed O1 and O2 positions occur in the aluminatesodalite.

The following is proposed for the transitions and modulations in aluminatesodalite. At high temperature, the $[\text{Ca}_4\text{CrO}_4]^{6+}$ clusters in the cubic aluminatesodalite are disordered, together with the framework O atoms, over the O1 and O2 positions above 610 K. The $[\text{Ca}_4\text{CrO}_4]^{6+}$ clusters are ordered and cause two-dimensional periodic APBs between 453 and 610 K. The APBs are accompanied by positional modulations of the framework O atoms on the O1 and O2 positions. Between 432 and 453 K, the $[\text{Ca}_4\text{CrO}_4]^{6+}$ clusters are ordered on fewer than the six

cubic orientations, and structural changes occur from the modulated structure to tetragonal symmetry. The tetragonal commensurate superstructure changes to an orthorhombic commensurate superstructure below 432 K with different ordering of the $[\text{Ca}_4\text{CrO}_4]^{6+}$ clusters on the six orientations. Either or both of the above transitions are associated with structural modulations. The transition from tetragonal to orthorhombic symmetry is associated with random transformation twins on a $\{110\}$ plane.

ACKNOWLEDGMENTS

The referees, G.L. Nord Jr. and P. Heaney, are thanked for helpful comments on this manuscript. John Barry is thanked for useful suggestions and for his help in using the 4000EX microscope. The aluminatesodalite sample was provided by Yohan DeVellier. This work was financially supported by a University of Kuwait grant SG-038 to I.H. and by NSF grant EAR-8708169 to P.R. Buseck; microscopy data were obtained at the Arizona State University HREM Facility and at the University of Kuwait EM Centre.

REFERENCES CITED

- Depmeier, W. (1988a) Aluminatesodalites: A family with strained structure and ferroic phase transitions. *Physics and Chemistry of Minerals*, 15, 419–426.
- (1988b) Structure of cubic aluminatesodalite $\text{Ca}_8[\text{Al}_{12}\text{O}_{24}](\text{WO}_4)_2$ in comparison with its orthorhombic phase and with cubic $\text{Sr}_8[\text{Al}_{12}\text{O}_{24}](\text{CrO}_4)_2$. *Acta Crystallographica*, B44, 201–207.
- Depmeier, W., Schmid, H., Setter, N., and Werk, M.L. (1987) Structure of cubic aluminatesodalite $\text{Sr}_8[\text{Al}_{12}\text{O}_{24}](\text{CrO}_4)_2$. *Acta Crystallographica*, C43, 2251–2255.
- Hassan, I. (1996a) Twinning in an orthorhombic aluminatesodalite, $\text{Ca}_8[\text{Al}_{12}\text{O}_{24}](\text{CrO}_4)_2$. *Mineralogical Magazine*, 60, 617–622.
- (1996b) Structural modulations in a pseudo-cubic aluminatesodalite, $\text{Ca}_8[\text{Al}_{12}\text{O}_{24}](\text{CrO}_4)_2$. *Zeitschrift für Kristallographie*, 211, 228–233.
- (1996c) Aluminatesodalite, $\text{Ca}_8[\text{Al}_{12}\text{O}_{24}](\text{CrO}_4)_2$, with tetragonal and orthorhombic superstructures. *European Journal of Mineralogy*, 8, 477–486.
- (1996d) Two-dimensional periodic antiphase boundaries (APBs) in a synthetic aluminatesodalite, $\text{Ca}_8[\text{Al}_{12}\text{O}_{24}](\text{CrO}_4)_2$. *Canadian Mineralogist*, 34, in press.
- Hassan, I., and Grundy, H.D. (1984) The crystal structures of sodalite-group minerals. *Acta Crystallographica*, B40, 6–13.
- Hassan, I., Peterson, R.C., and Grundy, H.D. (1985) The structure of lazurite, ideally $\text{Na}_4\text{Ca}_2(\text{Al}_6\text{Si}_6\text{O}_{24})\text{S}_2$, a member of the sodalite group. *Acta Crystallographica*, C41, 827–832.
- Hassan, I., and Buseck, P.R. (1988) A HRTEM characterization of scapolite solid-solutions. *American Mineralogist*, 73, 119–134.
- (1989a) Incommensurate-modulated structure of nosean, a sodalite-group mineral. *American Mineralogist*, 74, 394–410.
- (1989b) Cluster ordering and antiphase domain boundaries in hauyne. *Canadian Mineralogist*, 27, 173–180.
- Hassan, I., and Grundy, H.D. (1989) The structure of nosean, ideally $\text{Na}_8[\text{Al}_6\text{Si}_6\text{O}_{24}]\text{SO}_3 \cdot \text{H}_2\text{O}$. *Canadian Mineralogist*, 27, 165–172.
- (1991) The crystal structure of hauyne at 293 and 153 K. *Canadian Mineralogist*, 29, 123–130.
- Xu, H., and Veblen, D.R. (1995) Transmission electron microscopy study of optically anisotropic and isotropic hauyne. *American Mineralogist*, 80, 87–93.

MANUSCRIPT RECEIVED JUNE 27, 1995

MANUSCRIPT ACCEPTED JULY 8, 1996